

# Asymmetric Cherenkov acoustic reverse in topological insulators

Sergey Smirnov

*Institut für Theoretische Physik, Universität Regensburg, D-93040 Regensburg, Germany*

(Dated: September 16, 2014)

A general phenomenon of the Cherenkov radiation known in optics or acoustics of conventional materials is a formation of a forward cone of, respectively, photons or phonons emitted by a particle accelerated above the speed of light or sound in those materials. Here we suggest three-dimensional topological insulators as a unique platform to fundamentally explore and practically exploit the acoustic aspect of the Cherenkov effect. We demonstrate that applying an in-plane magnetic field to a surface of a three-dimensional topological insulator one may suppress the forward Cherenkov sound up to zero at a critical magnetic field. Above the critical field the Cherenkov sound acquires pure backward nature with the polar distribution differing from the forward one generated below the critical field. Potential applications of this asymmetric Cherenkov reverse are in design of low energy electronic devices such as acoustic ratchets or, in general, in low power design of electronic circuits with a magnetic field control of the direction and magnitude of the Cherenkov dissipation.

PACS numbers: 73.20.At, 63.20.kd, 41.60.Bq, 43.35.+d

## I. INTRODUCTION

The Cherenkov radiation discovered experimentally by Cherenkov<sup>1</sup> in optics of transparent media and theoretically explained later by Tamm and Frank<sup>2</sup> represents a general and important channel of energy dissipation. This kind of dissipation arises whenever fast particles propagate in media with which they interact via certain microscopic mechanisms. This dissipation mechanism is not restricted to only optical media where particles exciting photons have velocities in excess of the speed of light in those media. It also appears in solids where particles move faster than sound and, as a result, excite lattice vibrations or phonons. In both cases the photons or phonons are distributed within a forward cone centered around the momentum of the particle producing the Cherenkov light or sound.

Focusing on the Cherenkov sound, or the acoustic Cherenkov effect, one may distinguish three aspects particularly important in practice. The first aspect is related to energy losses in electronic devices. Indeed, in any solid electrons are coupled to the lattice. The strength of this coupling is temperature independent. Therefore, at any temperature fast electrons emit phonons, *i.e.*, lose their energy via the Cherenkov dissipation limiting in this way the efficiency of devices. The second aspect of the acoustic Cherenkov effect is its use in building acoustic devices. Here implementations include acoustic amplifiers based on Si/SiGe/Si heterostructures<sup>3</sup>, the GaAs technology<sup>4</sup>, piezoelectric semiconductors<sup>5</sup> as well as terahertz sound sources based on graphene<sup>6</sup>. Finally, the third aspect of the Cherenkov sound consists in investigation of the properties of the media where it propagates because the character of the Cherenkov sound strongly depends on these properties. This aspect of the Cherenkov sound has been, *e.g.*, exploited in Ref. 7 to study properties of ultracold Bose gases.

In the above first two practical aspects of the Cherenkov acoustic effect it is essential to have a, possi-

bly, simple control over the magnitude and direction of the generated sound. In particular, for the device efficiency it is crucial to reduce the energy losses and it is thus attractive to get an external access to the Cherenkov radiation with the possibility to completely close this dissipation channel. Alternatively, an external control is invaluable to direct the Cherenkov sound along specific directions and block its propagation in some others. In this situation one meets a fundamental problem of overcoming the forward Cherenkov cone which in an optical setup has been addressed in Ref. 8 within photonic crystals. In these systems a possibility to generate pure backward Cherenkov light has been demonstrated at the expense of the system's spatial inhomogeneity. Also an acoustic implementation of backward Cherenkov sound has been explored in electronic systems with spin-orbit interactions which is particularly appealing for future spintronic devices. For example, in two-dimensional electron gases with the Bychkov-Rashba<sup>9</sup> spin-orbit interaction interchiral transitions are responsible for the generation of the sound outside<sup>10</sup> the Cherenkov cone. The strong spin-orbit interaction in topological insulators<sup>11,12</sup> and the helical<sup>13,14</sup> nature of their surface states offer an alternative<sup>15</sup> possibility to generate backward Cherenkov sound due to only intrachiral transitions between the anisotropic<sup>16</sup> surface helical states.

The Cherenkov sound in these spin-orbit coupled systems represents fundamental interest and can be exploited to study the properties of these systems. However, its practical use in electronic devices could be limited because of some drawbacks. First, although backward Cherenkov sound appears, it is not pure because together there always appears forward Cherenkov sound. Second, the magnitude of the Cherenkov sound is fixed by the system parameters which are difficult or even impossible to switch during device operation. Additionally, in the case of topological insulators the required anisotropy of the helical surface states starts to play a role at rather large energies and momenta. This could limit the use

of the anisotropy in applications of topological insulators in the future generation of integrated electronic circuits operating at low energies.

To avoid the above mentioned drawbacks we propose in this paper a simple way to externally control the Cherenkov dissipation by means of an in-plane magnetic field. For this type of control surface helical states of three-dimensional topological insulators turn out to be most suitable especially at low energies relevant for applications of topological insulators in low power design electronics. One of the relevant device applications we discuss is an acoustic ratchet. This acoustic spin-orbit ratchet may be considered as a phonon alternative to the electron spin-orbit ratchet proposed in Ref. 17 within a two-dimensional Bychkov-Rashba electron gas.

The paper is organized as follows. In Section II we qualitatively describe the picture of the Cherenkov acoustic reverse where the forward sound reverses to the backward one when an in-plane magnetic field exceeds a critical value. The actual polar distribution of the forward and backward Cherenkov sound is found in Section III where we demonstrate that the Cherenkov reverse has an asymmetric character. We further explain the physical reason of this asymmetry and suggest to use it in electronic devices such as acoustic ratchets. In Section IV we conclude the paper.

## II. CHERENKOV REVERSE ON A SURFACE OF A THREE-DIMENSIONAL TOPOLOGICAL INSULATOR

The low energy surface helical states of a three-dimensional topological insulator are described by the Dirac Hamiltonian,

$$\hat{H}_0 = v(\hat{p}_x \hat{\sigma}_y - \hat{p}_y \hat{\sigma}_x), \quad (1)$$

where  $v$  is the Dirac velocity and  $\hat{p}_i$ ,  $\hat{\sigma}_i$ ,  $i = x, y$ , are the momentum and spin operators. The important difference of this Dirac Hamiltonian from the one describing graphene<sup>18</sup> is that in Eq. (1) the particle momentum is coupled to the real spin and not to the pseudo-spin describing the lattice degree of freedom in graphene.

Exactly this circumstance provides an opportunity to control the Cherenkov dissipation in a three-dimensional topological insulator applying an in-plane magnetic field to its surface. Indeed, such a field is described by the Zeeman contribution  $\hat{H}_Z$  to the total Hamiltonian,

$$\begin{aligned} \hat{H} &= \hat{H}_0 + \hat{H}_Z, \\ \hat{H}_Z &= \frac{1}{2} g \mu_B \hat{\sigma} \mathbf{H}, \end{aligned} \quad (2)$$

where  $g$  is the  $g$ -factor,  $\mu_B$  is the Bohr magneton,  $\hat{\sigma} = \mathbf{i}\hat{\sigma}_x + \mathbf{j}\hat{\sigma}_y$  and  $\mathbf{H} = \mathbf{i}H_x + \mathbf{j}H_y$ . Therefore, the position of the Dirac point, which is the minimum of the conduction band and the maximum of the valence band, becomes

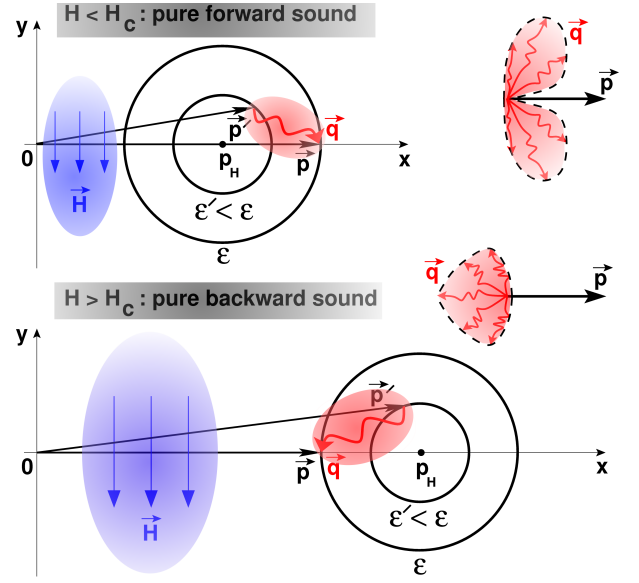


FIG. 1. The schematic picture of the Cherenkov acoustic reverse on a surface of a three-dimensional topological insulator subject to an in-plane magnetic field. The helical particle's momentum and energy before exciting the Cherenkov sound are  $\mathbf{p}$  (black thick horizontal arrows) and  $\epsilon$  while after emitting a phonon with momentum  $\mathbf{q}$  (red wavy arrows) they become  $\mathbf{p}'$  (black thick inclined arrows) and  $\epsilon'$ . An in-plane magnetic field (blue vertical arrows) is applied in the direction opposite to the  $y$ -axis. The black circles represent low energy isotropic surfaces of constant energy given by Eq. (3). Their center  $p_H$  (black dot) is the magnetic field dependent Dirac point. In the upper part  $p_H < |\mathbf{p}|$  resulting in pure forward Cherenkov sound. In the lower part  $p_H > |\mathbf{p}|$ . In this case the Cherenkov sound reverses and acquires pure backward nature. In both cases the Cherenkov sound distribution is shown as the shaded red area with phonon momenta  $\mathbf{q}$  (red wavy arrows) inside.

magnetic field dependent as can be seen from the energy-momentum dispersion relation,

$$\begin{aligned} \epsilon_\mu(\mathbf{p}) &= \mu \left[ v^2 \mathbf{p}^2 + v |\mathbf{p}| g \mu_B |\mathbf{H}| \sin(\phi_{\mathbf{H}} - \theta_{\mathbf{p}}) + \right. \\ &\quad \left. + \left( \frac{1}{2} g \mu_B |\mathbf{H}| \right)^2 \right]^{\frac{1}{2}}, \end{aligned} \quad (3)$$

where  $\mu = \pm 1$  is the chiral index (+1-conduction band, -1-valence band),  $\phi_{\mathbf{H}}$  and  $\theta_{\mathbf{p}}$  are, respectively, the angles of the in-plane magnetic field and the helical particle momentum with respect to the  $x$ -axis.

In topological insulators the Dirac velocity  $v$  is usually much larger than the sound velocity  $c$ . For example, for  $\text{Bi}_2\text{Te}_3$  these velocities are  $v \approx 3.87 \times 10^5$  m/s and  $c \approx 2.84 \times 10^3$  m/s. The relation  $v \gg c$  implies<sup>15</sup> that the Cherenkov sound may be generated only due to transitions  $|\mathbf{p}\mu\rangle \rightarrow |\mathbf{p}'\mu'\rangle$  with  $\mu = \mu'$ .

These two remarkable features specific to topological insulators, the magnetic field shift of the Dirac point and the intrachiral nature of the Cherenkov sound, pro-

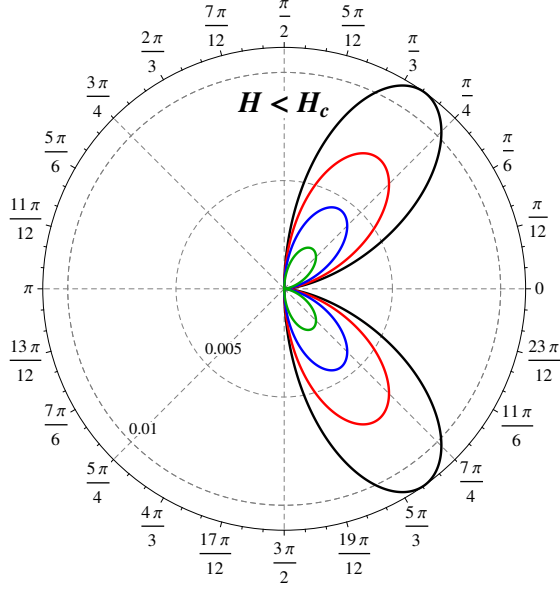


FIG. 2. The polar distributions of the Cherenkov sound intensity  $W(\phi)$  on a surface of  $\text{Bi}_2\text{Te}_3$  for the case  $|\mathbf{H}| < H_c$ . The magnitude of the helical particle momentum  $|\mathbf{p}| = 4.05 \times 10^{-27}$  is chosen to be small to stay within low energies well captured by the Dirac isotropic model. The polar distributions correspond to different magnitudes of the magnetic field, *i.e.*, to different values of the parameter  $h$ : 0.0 (black), 50.0 (red), 100.0 (blue), 150.0 (green). The critical value of  $h$  corresponding to  $H_c$  is  $h_c = 272.0$ . The Cherenkov sound is purely forward for all  $h < h_c$ . When  $h$  increases,  $W(\phi)$  decreases and totally vanishes at  $h = h_c$ .

vide a simple possibility for an external control of the Cherenkov dissipation.

To qualitatively explain the idea let us consider the Cherenkov sound excited by a helical particle in the conduction band. The particle has energy  $\varepsilon$  and momentum  $\mathbf{p}$  along the  $x$ -axis ( $\theta_{\mathbf{p}} = 0$ ). An in-plane magnetic field is applied perpendicular to the vector  $\mathbf{p}$  ( $\phi_{\mathbf{H}} = -\pi/2$ ). As demonstrated in Fig. 1, the low energy Dirac-like isotropic character of the constant energy surfaces does not change in the presence of an in-plane magnetic field which only shifts the Dirac point from zero to  $p_H$ . The Dirac point is a special point of the helical particle energy-momentum dependence, Eq. (3), and tuning the magnitude of the magnetic field to the critical value  $|\mathbf{H}| = H_c$ , such that  $p_H = |\mathbf{p}|$ , changes the behavior of the system. Indeed, as one can see from Fig. 1, in the case  $|\mathbf{H}| < H_c$  one has  $p_H < |\mathbf{p}|$  and the momentum  $\mathbf{p}$  of the helical particle exciting the Cherenkov sound touches the corresponding constant energy surface from the inside of the Dirac cone. In such a situation the energy and momentum conservation admits only such helical particle's final states, characterized by energy  $\varepsilon'$  and momentum  $\mathbf{p}'$ , which result in purely forward Cherenkov sound located inside the Cherenkov cone. On the other side, when  $|\mathbf{H}| > H_c$ , the Dirac point satisfies  $p_H > |\mathbf{p}|$  and one is

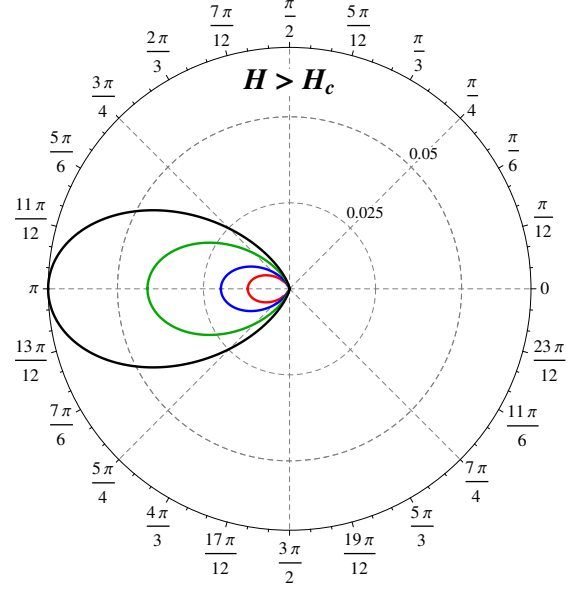


FIG. 3. The polar distributions of the Cherenkov sound intensity  $W(\phi)$  on a surface of  $\text{Bi}_2\text{Te}_3$  for the case  $|\mathbf{H}| > H_c$ . The helical particle momentum is the same as for Fig. 2. The polar distributions correspond to  $h = 450.0$  (red), 500.0 (blue), 600.0 (green), 700.0 (black). The Cherenkov sound is of pure backward nature for all  $h > h_c$ .

in the situation where  $\mathbf{p}$  touches the constant energy surface from the outside of the Dirac cone. As shown in Fig. 1, under such circumstances the energy and momentum conservation reverts the Cherenkov sound placing it outside the Cherenkov cone, *i.e.*, enforces it to acquire pure backward nature.

### III. TWO-DIMENSIONAL DISTRIBUTION OF THE FORWARD AND BACKWARD CHERENKOV SOUND

To quantitatively verify this picture and to find out the actual distribution of the Cherenkov sound and its dependence on the in-plane magnetic field we calculate the imaginary part of the self-energy describing the interaction<sup>19</sup> between helical particles and phonons,

$$\begin{aligned} \hat{H}_{\text{ph}} &= \sum_{\mathbf{k}} \hbar\omega(\mathbf{k})(b_{\mathbf{k}}^\dagger b_{\mathbf{k}} + 1/2), \\ \hat{H}_{\text{el-ph}} &= g_{ph} \sum_{\sigma} \int d\mathbf{r} \hat{\psi}_{\sigma}^\dagger(\mathbf{r}) \hat{\psi}_{\sigma}(\mathbf{r}) \hat{\varphi}(\mathbf{r}), \\ \hat{\varphi}(\mathbf{r}) &= i \sum_{\mathbf{k}} \sqrt{\frac{\hbar\omega(\mathbf{k})}{2V}} \left[ \exp\left(i\frac{\mathbf{k}\mathbf{r}}{\hbar}\right) b_{\mathbf{k}} - h.c. \right]. \end{aligned} \quad (4)$$

In Eq. (4)  $b_{\mathbf{k}}^\dagger$ ,  $b_{\mathbf{k}}$  are the phonon creation and annihilation operators, respectively, the phonon spectrum is  $\hbar\omega(\mathbf{k}) = c|\mathbf{k}|$ ,  $g_{ph}$  is the strength of the coupling to phonons,  $V$  is

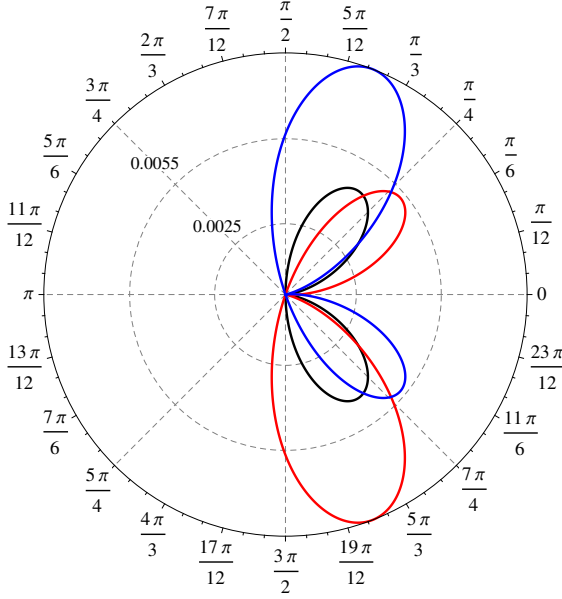


FIG. 4. The polar distributions of the Cherenkov sound intensity  $W(\phi)$  on a surface of  $\text{Bi}_2\text{Te}_3$  for the case  $|\mathbf{H}| < H_c$ . The helical particle momentum is the same as for Fig. 2. The polar distributions correspond to  $h = 100.0$  and  $\phi_{\mathbf{H}} = -\pi/2$  (black),  $\phi_{\mathbf{H}} = -\pi/4$  (red) and  $\phi_{\mathbf{H}} = -3\pi/4$  (blue). The Cherenkov sound is mainly forward but narrow backward angular sectors appear for  $\phi_{\mathbf{H}} = -\pi/4$  and  $\phi_{\mathbf{H}} = -3\pi/4$ .

the volume and  $\hat{\psi}_\sigma^\dagger(\mathbf{r})$ ,  $\hat{\psi}_\sigma(\mathbf{r})$  are, respectively, the helical particle creation and annihilation field operators.

In the second order in  $g_{ph}$  a derivation similar to the ones in Refs. 10, 15, and 20 allows one to represent the imaginary part of the self-energy  $\Sigma(\epsilon_{\mathbf{p}+})$  in the form

$$\text{Im}[\Sigma(\epsilon_{\mathbf{p}+})] = -\frac{g_{ph}^2 \mathbf{p}^2}{8\pi\hbar^3} \int_{-\pi}^{\pi} d\phi W(\phi), \quad (5)$$

where  $W(\phi)$  is the polar distribution of the Cherenkov sound. It can be written as the sum,

$$W(\phi) = \sum_i x_i^2(\phi) f_1[x_i(\phi), \phi] f_2[x_i(\phi), \phi], \quad (6)$$

over all roots of the energy-momentum conservation equation,

$$\begin{aligned} & \sqrt{\left(\frac{v}{c}\right)^2 + \frac{v}{c} h \sin(\phi_{\mathbf{H}}) + \frac{h^2}{4}} - \\ & - \sqrt{\left(\frac{v}{c}\right)^2 f_3(x, \phi) + \frac{v}{c} h f_4(x, \phi) + \frac{h^2}{4}} - x = 0, \end{aligned} \quad (7)$$

where the physical meaning of  $x$  is the ratio  $|\mathbf{q}|/|\mathbf{p}|$  between the magnitudes of the phonon and helical particle

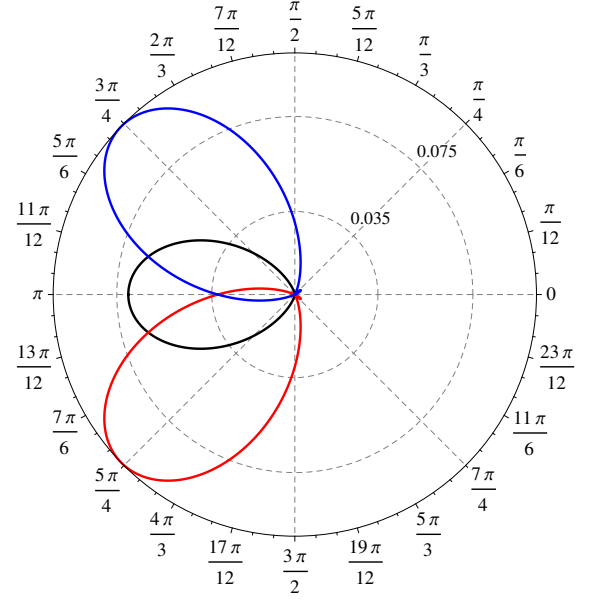


FIG. 5. The polar distributions of the Cherenkov sound intensity  $W(\phi)$  on a surface of  $\text{Bi}_2\text{Te}_3$  for the case  $|\mathbf{H}| > H_c$ . The helical particle momentum is the same as for Fig. 2. The polar distributions correspond to  $h = 700.0$  and  $\phi_{\mathbf{H}} = -\pi/2$  (black),  $\phi_{\mathbf{H}} = -\pi/4$  (red) and  $\phi_{\mathbf{H}} = -3\pi/4$  (blue). The Cherenkov sound is mainly backward but narrow forward angular sectors appear for  $\phi_{\mathbf{H}} = -\pi/4$  and  $\phi_{\mathbf{H}} = -3\pi/4$ .

momenta. In Eq. (6) the functions  $f_{1,2}(x, \phi)$  are

$$\begin{aligned} f_1(x, \phi) &= \\ &= \frac{1}{2} \left( 1 + \frac{\frac{v}{c}(1 - x \cos(\phi)) + \frac{1}{2}h \sin(\phi_{\mathbf{H}})}{\sqrt{\left(\frac{v}{c}\right)^2 f_3(x, \phi) + \frac{v}{c} h f_4(x, \phi) + \frac{h^2}{4}}} \right), \\ f_2(x, \phi) &= \\ &= \left[ 1 + \frac{\left(\frac{v}{c}\right)^2 f_3'(x, \phi) + \frac{v}{c} h f_4'(x, \phi)}{2\sqrt{\left(\frac{v}{c}\right)^2 f_3(x, \phi) + \frac{v}{c} h f_4(x, \phi) + \frac{h^2}{4}}} \right]^{-1}, \end{aligned} \quad (8)$$

where  $f'(x, \phi) \equiv \partial_x f(x, \phi)$ . In Eqs. (7) and (8) the quantity  $h$  is defined as  $h \equiv g\mu_B |\mathbf{H}|/pc$  and the functions  $f_{3,4}(x, \phi)$  are

$$\begin{aligned} f_3(x, \phi) &= 1 + x^2 - 2x \cos(\phi), \\ f_4(x, \phi) &= \sin(\phi_{\mathbf{H}}) + x \sin(-\phi_{\mathbf{H}} + \phi). \end{aligned} \quad (9)$$

In Fig. 2 the polar distribution of the Cherenkov sound intensity  $W(\phi)$  on a surface of the three-dimensional topological insulator  $\text{Bi}_2\text{Te}_3$  is shown for the situation depicted in Fig. 1. Different values of  $h$  correspond to the magnetic field magnitude such that  $|\mathbf{H}| < H_c$ . The critical value  $H_c = 2|\mathbf{p}|v/g\mu_B$  is obtained from the condition  $p_H = |\mathbf{p}|$  where  $p_H = g\mu_B |\mathbf{H}|/2v$ . The value of  $|\mathbf{p}| = 4.05 \times 10^{-27} \text{ kg}\cdot\text{m/s}$  is chosen to be small enough so that the isotropic Dirac cone describes well<sup>16</sup> the energy-momentum dependence, Eq. (3). Taking the  $g$ -factor

from Ref. 21,  $g \approx 20$ , we obtain for  $h = 0.0, 50.0, 100.0, 150.0$  the magnitude of the magnetic field in Tesla,  $|\mathbf{H}| = 0.0\text{T}, 3.1\text{T}, 6.2\text{T}, 9.3\text{T}$ , respectively. From Fig. 2 it is clear that the Cherenkov sound is purely forward for all  $|\mathbf{H}| < H_c$ . With the increase of the magnetic field magnitude the intensity of the Cherenkov sound decreases. At the critical field  $H_c = 16.9\text{T}$  the Cherenkov dissipation fully disappears, *i.e.*,  $W(\phi) = 0$ , for all angles,  $-\pi \leq \phi < \pi$ .

The Cherenkov sound distribution for larger fields,  $|\mathbf{H}| > H_c$ , is shown in Fig. 3. Here  $h = 450.0, 500.0, 600.0, 700.0$  which correspond to  $H = 27.9\text{T}, 31.0\text{T}, 37.2\text{T}, 43.4\text{T}$ . As expected from our qualitative discussion, at  $|\mathbf{H}| > H_c$  the Cherenkov sound is of pure backward nature. Note that the maximum of the backward sound intensity is at  $\phi = \pm\pi$  which corresponds to strictly backward sound. This means that at large magnetic fields helical particles mainly scatter strictly forward thus keeping the tendency to produce backward sound in subsequent scattering unless they finally reach the Dirac point  $p_H$ .

For completeness we also present results for  $\phi_{\mathbf{H}} \neq -\pi/2$ . In Fig. 4 we show the Cherenkov sound distribution for the case  $|\mathbf{H}| < H_c$  while in Fig. 5 it is shown for the case  $|\mathbf{H}| > H_c$ . In both cases the symmetry of the angular distribution of the Cherenkov sound breaks and it is no longer of pure forward or backward nature as it was for  $\phi_{\mathbf{H}} = -\pi/2$  shown as the black curves in Figs. 4 and 5, respectively. In addition to the forward and backward Cherenkov sound narrow angular droplets of the backward and forward sound can be seen in Figs. 4 and 5, respectively.

Finally, we would like to emphasize the asymmetry between the forward and backward distributions. In particular, as shown in Ref. 15, the strictly forward sound is absent, as can be seen in Fig. 2. At the same time the strictly backward sound in Fig. 3 is maximal. The physical reason for this asymmetry lies in the helical nature of the particles on a surface of a three-dimensional topological insulator. More precisely, the spinorial structure of these states has a strong dependence on the momentum orientation and the sound distribution depends on the mutual orientation between the momentum  $\mathbf{p}$  and the group velocity  $\mathbf{v}_g$ . The forward and backward sound defined with respect to the momentum  $\mathbf{p}$  is, of course, always forward with respect to the group velocity  $\mathbf{v}_g$ . However, due to the helical structure of the surface states, the sound distribution has distinct shapes depending on whether the vectors  $\mathbf{p}$  and  $\mathbf{v}_g$  are parallel or antiparallel.

This asymmetry suggests an experimental challenge

for an implementation of an electronic device such as an acoustic ratchet. In this device the magnitude of a periodic in-plane magnetic field slowly changes from zero up to some maximal value  $H_{max} > H_c$  and back to zero. During this period no strictly forward sound will be produced by helical particles with a fixed momentum whereas they will produce the strictly backward sound. Thus a directed phonon flow in the direction opposite to the  $x$ -axis will be created.

#### IV. CONCLUSIONS

In conclusion, the Cherenkov sound excited on a surface of a three-dimensional topological insulator may be effectively controlled by an in-plane magnetic field. Applying such a field perpendicular to the helical particle propagation suppresses the Cherenkov dissipation up to zero at a critical field. For larger fields the Cherenkov sound asymmetrically reverses its direction and acquires pure backward nature.

The magnetic field shift of the conduction/valence band minimum/maximum in the momentum space and the dependence of the spinorial structure of the helical particles on the momentum orientation, are specific to three-dimensional topological insulators and do not have counterparts in conventional systems where under the Zeeman split the energy bands shift along the energy axis but not in the momentum space. As a result, the Cherenkov sound on a surface of a three-dimensional topological insulator in an in-plane magnetic field is a unique physical phenomenon totally distinct from what has been known about the Cherenkov radiation in conventional materials without and with magnetic field as well as in three-dimensional topological insulators without magnetic field.

This unique behavior occurs at low energies and, thus, of practical relevance in the control of the energy dissipation in future low power design electronics based on topological insulators as well as in building different acoustic devices, in particular, acoustic ratchets generating directed sound flows.

#### V. ACKNOWLEDGMENTS

Support from the DFG under the program SFB 689 is acknowledged.

<sup>1</sup> P. A. Cherenkov, Doklady Akad. Nauk SSSR **2**, 451 (1934).

<sup>2</sup> I. E. Tamm and I. M. Frank, Doklady Akad. Nauk. SSSR **14**, 107 (1937).

<sup>3</sup> S. M. Komirenko, K. W. Kim, A. A. Demidenko, V. A. Kochelap, and M. A. Strosio, Appl. Phys. Lett. **76**, 1869

(2000).

<sup>4</sup> X. F. Zhao, J. Zhang, S. M. Chen, and W. Xu, J. Appl. Phys. **105**, 104514 (2009).

<sup>5</sup> M. Willatzen and J. Christensen, Phys. Rev. B **89**, 041201(R) (2014).

- <sup>6</sup> C. X. Zhao, W. Xu, and F. M. Peeters, Appl. Phys. Lett. **102**, 222101 (2013).
- <sup>7</sup> D. L. Kovrizhin and L. A. Maksimov, Phys. Lett. A **282**, 421 (2001).
- <sup>8</sup> C. Luo, M. Ibanescu, S. G. Johnson, and J. D. Joannopoulos, Science **299**, 368 (2003).
- <sup>9</sup> Y. A. Bychkov and E. I. Rashba, JETP Letters **39**, 78 (1984).
- <sup>10</sup> S. Smirnov, Phys. Rev. B **83**, 081308(R) (2011).
- <sup>11</sup> M. Z. Hasan and C. L. Kane, Rev. Mod. Phys. **82**, 3045 (2010).
- <sup>12</sup> X.-L. Qi and S.-C. Zhang, Rev. Mod. Phys. **83**, 1057 (2011).
- <sup>13</sup> C. Wu, B. A. Bernevig, and S.-C. Zhang, Phys. Rev. Lett. **96**, 106401 (2006).
- <sup>14</sup> C. Xu and J. E. Moore, Phys. Rev. B **73**, 045322 (2006).
- <sup>15</sup> S. Smirnov, Phys. Rev. B **88**, 205301 (2013).
- <sup>16</sup> L. Fu, Phys. Rev. Lett. **103**, 266801 (2009).
- <sup>17</sup> S. Smirnov, D. Bercioux, M. Grifoni, and K. Richter, Phys. Rev. Lett. **100**, 230601 (2008).
- <sup>18</sup> A. H. Castro Neto, F. Guinea, N. M. R. Peres, K. S. Novoselov, and A. K. Geim, Rev. Mod. Phys. **81**, 109 (2009).
- <sup>19</sup> A. A. Abrikosov, L. P. Gorkov, and I. E. Dzyaloshinski, *Methods of Quantum Field Theory in Statistical Physics* (Dover, New York, 1963).
- <sup>20</sup> L. S. Levitov and A. V. Shitov, *Green's Functions. Problems and Solutions*, 2nd ed. (Fizmatlit, Moscow, 2003) in Russian.
- <sup>21</sup> C. W. Rischau, B. Leridon, B. Fauqué, V. Metayer, and C. J. van der Beek, Phys. Rev. B **88**, 205207 (2013).